Fabrication and characterization of bit-patterned media beyond 1.5 Tbit/in^2

2011 Nanotechnology 22 385301

(http://iopscience.iop.org/0957-4484/22/38/385301)

Nanotechnology **22** (2011) 385301 (6pp) doi:10.1088/0957-4484/22/38/385301

Fabrication and characterization of bit-patterned media beyond 1.5 Tbit/in^2

Joel K W Yang[1], Yunjie Chen[2,4], Tianli Huang[2], Huigao Duan[1], Naganivetha Thiyagarajah[3], Hui Kim Hui[1], Siang Huei Leong[2] and Vivian Ng[3]

[1] Institute of Materials Research and Engineering, A*STAR, 3 Research Link, 117602, Singapore
[2] Data Storage Institute, A*STAR, 5 Engineering Drive, 117608, Singapore
[3] Department of Electrical and Computer Engineering, National University of Singapore, 4 Engineering Drive 3, 117576, Singapore

E-mail: yangkwj@imre.a-star.edu.sg and elengv@nus.edu.sg

Received 11 June 2011, in final form 15 July 2011
Published 25 August 2011
Online at stacks.iop.org/Nano/22/385301

Abstract
We fabricated bit-patterned media (BPM) at densities as high as 3.3 Tbit/in^2 using a process consisting of high-resolution electron-beam lithography followed directly by magnetic film deposition. By avoiding pattern transfer processes such as etching and liftoff that inherently reduce pattern fidelity, the resolution of the final pattern was kept close to that of the lithographic step. Magnetic force microscopy (MFM) showed magnetic isolation of the patterned bits at 1.9 Tbit/in^2, which was close to the resolution limit of the MFM. The method presented will enable studies on magnetic bits packed at ultra-high densities, and can be combined with other scalable patterning methods such as templated self-assembly and nanoimprint lithography for high-volume manufacturing.

S Online supplementary data available from stacks.iop.org/Nano/22/385301/mmedia

(Some figures in this article are in colour only in the electronic version)

As the hard disk drive (HDD) industry continues to increase the recording densities in future products, new methods for miniaturizing the magnetic bit are required. Current HDDs rely on advanced sputter deposition of alloys (e.g. Co, Cr, Pt) onto disk platters resulting in granular media, which consists of weakly-coupled magnetic grains ∼7–9 nm in size. Areal recording densities of ∼0.5 Tbit/in^2 are achieved where a single bit of information is stored over an area consisting of tens of these grains. To pack even more bits per unit area, one can logically either reduce the number of grains per bit, or the grain size. However, the lower limit for the number of grains per bit is set by the signal-to-noise-ratio requirements for data retrieval. On the other hand, the superparamagnetic limit [1] dictates the minimum grain size below which thermal instability of the magnetization state occurs. Hence, it is predicted that the areal recording density in granular media will not extend beyond ∼1–1.5 Tbit/in^2 [2, 3].

[4] Present address: Western Digital Singapore, 3 Tuas Link 2, 638552, Singapore.

In contrast, bit-patterned media (BPM) [1, 3–8] holds promise for areal recording densities in excess of 1.5 Tbit/in^2. In BPM, signal-to-noise ratio is significantly improved by lithographically patterning ordered arrays of magnetic bits. Thus, a single switchable volume per bit is sufficient for data retrieval, with each bit comfortably far from the superparamagnetic limit. Recent BPM efforts have demonstrated areal recording densities comparable to state-of-the-art granular media [9–11]. However, as the lithographic patterning of magnetic bits incurs significant cost, demonstrations of BPM with areal recording densities greatly surpassing that of granular media is currently needed in viability studies of high-density BPM to meet future commercial HDD requirements.

To demonstrate BPM beyond ∼1.5 Tbit/in^2, high-resolution lithography [12, 13] and processing methods are required. Although top-down and self-assembly approaches are available that readily demonstrate pattern resolutions with ∼10 Tdot/in^2 [12, 14–17], current fabrication methods rely

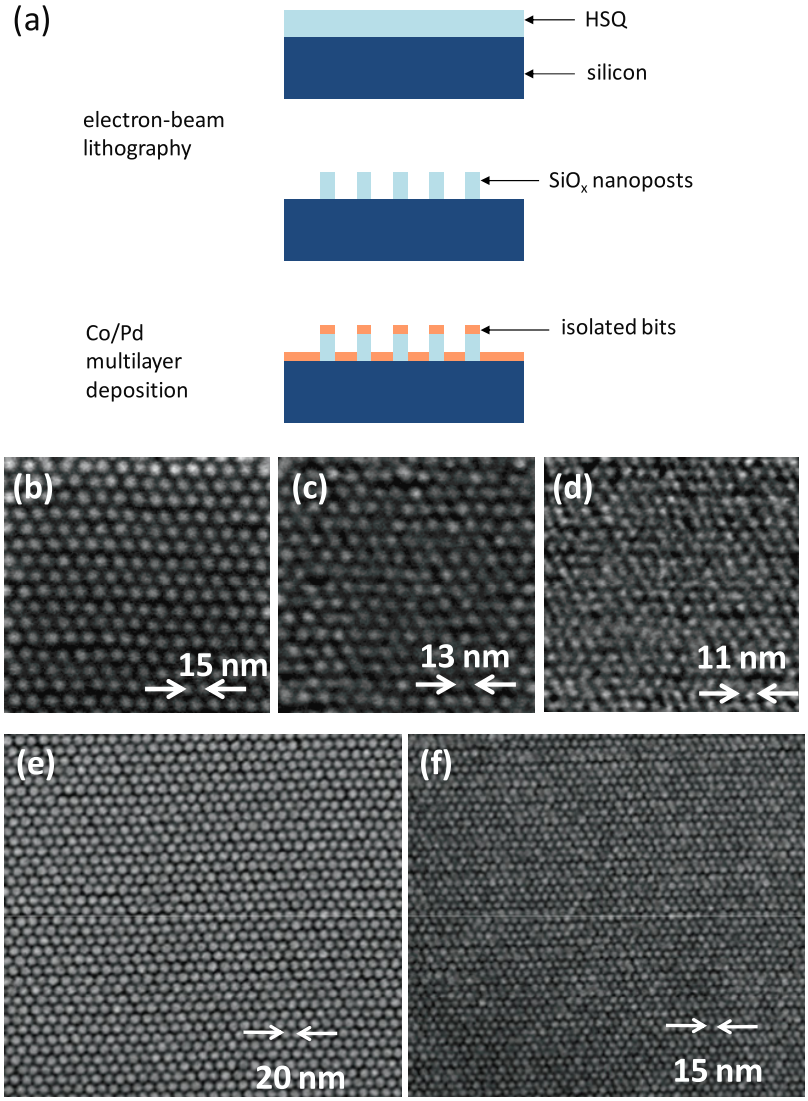

Figure 1. (a) Schematic of the two-step process used in fabricating high-density BPM. The process consists of high-resolution electron-beam lithography (EBL) of hydrogen silsesquioxane (HSQ) resist followed by magnetic film deposition using Co/Pd multilayers. (b)–(d) SEMs of patterned HSQ resist demonstrating the high-resolution capability of the EBL system and process. (e), (f) SEM images of magnetic bits at densities of 1.9 Tbit/in^2 (e) and 3.3 Tbit/in^2 (f) formed after depositing Co/Pd multilayers onto resist structures.

on pattern-transfer mechanisms such as etching and/or liftoff that degrade the resolution of the original pattern. Advances in etching techniques [18, 19] have shown promise in alleviating some of the problems with pattern transfer. However, preserving the resolution of the original patterns remains a fundamental challenge in achieving the highest possible bit densities [20].

In this paper, we present a process that achieves high-density patterned bits without needing to pattern transfer, hence reducing the number of steps from the initial pattern definition to media formation. This process as shown in figure 1(a) consists of (1) electron-beam lithography, followed by (2) Co/Pd multilayer film deposition. In contrast to prior work where magnetic films were deposited onto substrates that were pre-patterned by etching [9, 11, 20], we instead avoided etching steps to achieve higher-density BPM. The final structures are magnetically isolated bits on nanoposts of SiO_x resist. Although electron-beam lithography was used to demonstrate the high-resolution capability of this process, this approach can also be applied to other methods of pattern formation that are both high-resolution and scalable to large areas, such as guided self-assembly [17, 21, 22] and nanoimprint lithography [23, 24]. This approach allows the number of processing steps to be reduced, hence lowering the cost of disk media fabrication while providing a means to higher areal recording densities.

Hydrogen silsesquioxane (HSQ) resist in combination with the salty-development method was used in the high-resolution electron-beam lithography process [12, 25]. Details of this process can also be found in the supporting information (available at stacks.iop.org/Nano/22/385301/mmedia). Unlike organic resists, electron-beam-exposed HSQ results in a thermally and mechanically robust, and chemically stable (non-stoichiometric) silicon oxide (SiO_x), which is a durable

and suitable material for incorporation into HDD platters. Figures 1(b)–(d) show scanning electron micrograph (SEM) images of the hexagonal close-packed arrays of dots patterned in HSQ at pitches (densities) of 15 nm (3.3 Tdot/in^2), 13 nm (4.4 Tdot/in^2), and 11 nm (6.2 Tdot/in^2). The resolution of the lithography was high, with clearly defined sub-10 nm dots. However, the quality of the nanostructures decreased rapidly with increasing density, suggesting that we were operating close to the resolution limit of the tool/process. Note also the slight deviation of the dots from perfect lattice positions, especially in figures 1(c) and (d), that we attribute to noise during the exposure (waviness of horizontal rows), and capillary-force-induced cohesion [26] of posts during resist development (clustering of two or three posts). Hence, in the fabrication of magnetic bits, we limited our patterning density to 15 nm pitch (3.3 Tdot/in^2), to maintain adequate pattern quality.

Magnetic material was then deposited onto the resist topography to achieve magnetic bits with perpendicular anisotropy. Highly exchange-coupled Co/Pd or Co/Pt multilayer systems are ideal candidates for BPM applications due to their high perpendicular anisotropy and controllable magnetic properties [8, 9]. The perpendicular magnetic multilayer films with the structure [Co (0.3 nm)/Pd (0.9 nm)]$_8$ with an underlayer of Ta (5 nm)/Pd (3 nm) and a protection layer of Pd (3 nm) were deposited using dc-magnetron sputtering at room temperature. The magnetic properties of the continuous films were characterized by polar magneto-optic Kerr effect (MOKE) measurements with an external magnetic field applied normal to the sample. The continuous films were found to exhibit square hysteresis loops (indicative of highly-perpendicular magnetic anisotropy and strong exchange coupling) with a coercivity of below 1 kOe. The total thickness of this multilayer film structure was ∼21 nm. More details on magnetic film deposition can be found in the supporting information (available at stacks.iop.org/Nano/22/385301/mmedia).

SEM images of the patterned dots after media deposition are shown in figures 1(e) and (f) for dot pitches (densities) of 20 nm (1.9 Tbit/in^2) and 15 nm (3.3 Tbit/in^2). The magnetic bits were well defined and physically isolated. The visible gaps between adjacent bits were <5 nm, with a small fraction of bits that were physically connected. Though we see a higher fraction of interconnected bits at 3.3 Tbit/in^2, the majority of the bits were clearly isolated and well defined even at this density. As we show below, bits that are physically connected by thin magnetic links do remain magnetically isolated. Therefore, the patterned bits at 3.3 Tbit/in^2 are expected to be individually addressable, though direct evidence cannot be obtained due to limitations in existing characterization tools.

Due to the angled nature of the sputter deposition, the inter-shadowing effect of the nanoposts was expected to affect the profile, and the amount of magnetic material between of the magnetic bits. This effect was more clearly observed for structures at lower densities, as observed in the tilted-view SEM images in figures 2(a)–(d). It is clear, from the SEM images in figures 2(a) and (b), that prior to deposition the SiO_x nanoposts at pitches of 35 and 70 nm (both on the same substrate) were well isolated and uniform in shape and size. After media deposition the resulting bits were larger due to the coating of magnetic material on the structures, as shown in figures 2(c) and (d). The inter-shadowing of bits during the deposition was manifested in the taller and narrower profiles of the 35 nm-pitch bits compared to the 70 nm-pitch bits. Inter-shadowing hence suggests that more densely-packed bits would have less inter-bit magnetic material (i.e. magnetic material on the sidewall and substrate) than sparsely-packed bits. Another positive result of inter-shadowing was that the magnetic bits exhibited size uniformity independent of the initial HSQ nanopost sizes, as discussed in the supporting information (available at stacks.iop.org/Nano/22/385301/mmedia).

A transmission electron microscope (TEM) cross-sectional view of 30 nm-pitch magnetic bits is shown in figure 2(e) (see supporting information available at stacks.iop.org/Nano/22/385301/mmedia for details on sample preparation). The near-vertical sidewalls of the SiO_x nanoposts were evident in this TEM image, with magnetic-material deposition on all surfaces. Upon closer inspection, we see that the magnetic material was thickest on top of the posts, thinner on the substrate, and thinnest on the sidewalls. Although the magnetic bits on the posts were physically connected, they remarkably remained magnetically isolated and perhaps only weakly linked by the thin inter-bit magnetic material, similar to the results in [9]. Importantly, as densely-patterned bits will have less inter-bit magnetic material compared to sparsely-patterned bits, we expect and will show in the following that densely-packed bits (i.e. at 1.9 Tbit/in^2) do exhibit magnetic isolation. The effect of the inter-bit magnetic material on the performance of BPM will be the topic for future work.

To observe that the magnetic bits were magnetically isolated, independently magnetizable, and therefore have data storage capability, we performed magnetic force microscopy (MFM) after applying a uniform external magnetic field. As the bit density and coercivity of our patterned arrays were higher than those of commercial granular media, read/write tests using commercially-available HDD heads were not feasible. Nonetheless, with the following procedure, evidence of data storage potential can be obtained, as is commonly done [27]. Prior to MFM imaging, the samples were saturated by applying an *ex situ* large out-of-plane negative saturation field of ∼20 kOe. Uniform *ex situ* positive magnetic fields were then applied at set values and subsequently reduced to zero, thus leaving the patterned bits in their remanent states. MFM images of the remanent states were sequentially taken at different positive switching fields until all bits were magnetically reversed. Due to the finite switching field distribution in such systems, we were able to observe the switching of individual bits, indicative of magnetic isolation among the bits. More details of the MFM measurements of single bit-island reversal of patterned magnetic islands in BPM can be found in the supporting information (available at stacks.iop.org/Nano/22/385301/mmedia) and have also been described previously for lower-density bits [27–29].

The results from MFM characterization are shown in figure 3 for 35 nm-pitch bits corresponding to an areal

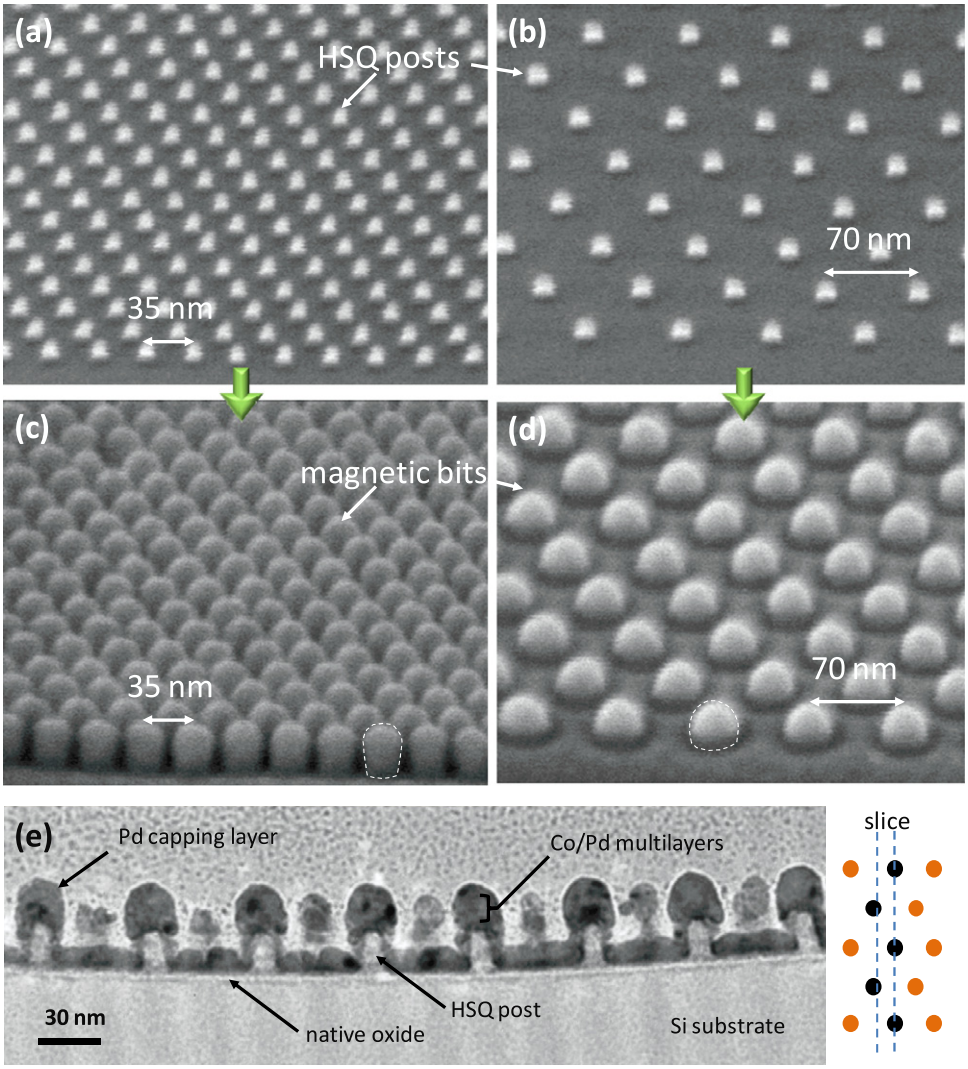

Figure 2. (a), (b) Tilted-view SEM images of the HSQ posts at 35 and 70 nm pitch prior to Co/Pd multilayer film deposition. (c), (d) SEM images of the resultant magnetic bits after Co/Pd multilayer film deposition onto the corresponding HSQ posts above. The dashed lines illustrate the differing side profiles of the isolated bits for the two pattern densities. (e) Bright-field TEM image showing the cross-sectional slice of a 30 nm-pitch array of magnetic bits. The inset is a schematic of the slice orientation and thickness relative to the hexagonal array.

recording density of 0.6 Tbit/in^2. Figures 3(a) and (b) show SEM and AFM images of the patterned array from which the series of representative MFM images in figure 3(c) were taken at different switching fields. At 35 nm pitch, the MFM resolution was sufficient to resolve individually switching bits, as can be seen in the five easy-switching bits that appear as bright spots in figure 3(c)(i). As these bits showed switching behavior that was independent of their neighboring bits, we expect that they would be individually switchable as well in a read/write experiment with an appropriate head. The normalized remanent magnetization (M_r) was calculated from the MFMs by counting the number of switched (bright) bits divided by the total number of bits in the array. Repeating the procedure with increasing switching fields (H) resulted in the M_r–H plot in figure 3(d). In contrast to coupled magnetic bits that exhibit a step increase in M_r, we observed instead a gradual increase with increasing H, which was a good indication of magnetically-isolated bits with a spread/distribution in switching fields. The mean coercivity of this array of bits was ∼8.5 kOe, while the switching field distribution (SFD) was ∼2 kOe. The increase in coercivity of patterned bits over that of an unpatterned film (<1000 Oe) was expected due to the different switching mechanisms in the continuous films (domain wall propagation) and the single-domain dots (Stoner–Wohlfarth-like switching) [10, 11].

Magnetic isolation of bits at 20 nm pitch (1.9 Tbit/in^2 density) is demonstrated next using a series of high-resolution MFM images in figure 4. The ability to resolve the magnetic bits at 20 nm pitch puts the resolution of our MFM capabilities at ∼10 nm half pitch, which is comparable to the best MFM resolution reported [30, 31]. SEM images of the patterned bits with regular bit sizes of ∼15 nm are shown in figure 4(a). The MFM images shown in figures 4(b) and (c) were taken at remanence after uniform switching fields of 13 550 Oe and 13 600 Oe respectively were applied. Each circular dark spot corresponds to a single unswitched bit. The features within the dashed rectangle in figure 4(b) are two unswitched bits closely spaced with a center-to-center distance of ∼35 nm as

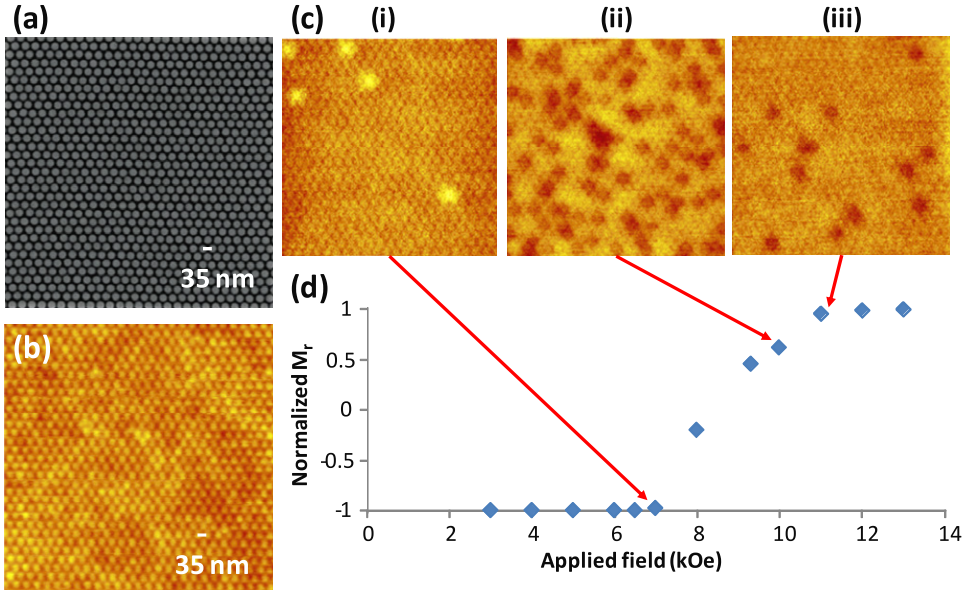

Figure 3. Magnetic force microscopy (MFM) characterization of patterned bits at 35 nm pitch (0.6 Tbit/in^2 density). (a), (b) SEM and AFM images of patterned magnetic bits. (c) MFM images after switching fields of progressively increasing strengths of 7 kOe (i), 10 kOe (ii), and 11 kOe (iii) were applied. (d) Normalized remanence curve obtained by calculating the fraction of switched bits (normalized M_r) plotted against the applied switching field. (Note: the topographical features of the patterned islands appear in the MFM images due to the increased non-magnetic short range tip–sample interactions because of the small tip scan height (∼10 nm) used during the MFM measurements.)

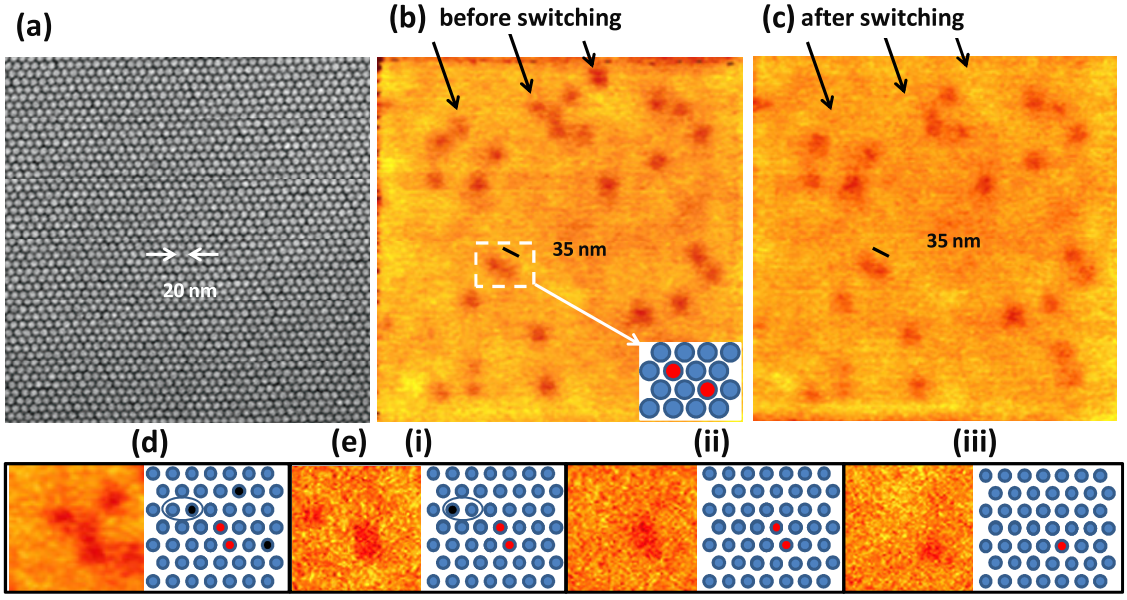

Figure 4. Evidence of magnetic isolation among bits patterned at 20 nm pitch corresponding to an areal density of 1.9 Tbit/in^2. (a) SEM image of the patterned array. (b), (c) Sequential MFM images of the corresponding partially switched magnetic bits imaged at remanence after switching fields of 13 550 Oe and 13 600 Oe respectively were applied. The dark spots indicate bits that remained unswitched. The arrows point to the bits that flipped their state due to the increase in switching field going from (b) to (c). The unswitched bits that were closely spaced at 35 nm center-to-center distance remain resolvable by MFM, as indicated by the scale bar and as red bits in the schematic inset. (d) Enlarged view of the top-center portion of the MFM image in (b) with the corresponding schematic showing the configuration of bits. (e) MFM images of bits in a repeat experiment after an increasing positive field was applied gradually from (i) 13 650 Oe to (ii) 13 775 Oe to (iii) 13 805 Oe, demonstrating the independent switching of individual bits.

represented schematically in the inset. With the small step of 50 Oe in applied field, three bits were observed to switch, as indicated by the arrows. The simultaneous switching of these bits due to a uniformly-applied switching field suggested that they each had similar coercivities and were magnetically isolated from their surrounding bits. If the bits were instead not isolated but magnetically coupled, large clusters of adjacent bits would be observed to switch together. However, repeated measurements at small steps in switching fields showed similar switching of other individual bits, with no clustering of bits.

For further evidence of magnetic isolation between neighboring bits, we repeated the experiments, concentrating on only a small number of bits, as shown in figure 4(d). Figure 4(d) is an enlarged view of the top portion of the MFM in figure 4(b) next to a schematic of the corresponding configuration of bits (blue = switched bits, red and black = unswitched bits). The experiment was repeated by reverse saturating the bits and reapplying gradually-increasing fields in the positive direction (figures 4(e)(i)–(iii)). The red dots in the schematic indicate the unswitched bits that are common between figures 4(d) and (e). The configurations of unswitched bits (black dots) in figures 4(d) and (e) are otherwise different in repeated experiments due to the small differences in switching fields (13 500 Oe in (d) and 13 650 Oe in (e)), and the non-deterministic nature of the switching of bits in a uniform applied field, as has been previously observed [29]. On close inspection, we see that the circled bits in figures 4(d) and (e)(i) form a pair of direct neighbors that swapped their switching sequence when the experiment was repeated, i.e. the left bit switched earlier than the right bit in the first experiment, and this sequence was reversed in the repeat experiment. This result provides further evidence that individual bits can be switched independently of their neighbors, which is essential for data storage. Going from figures 4(e)(ii) and (iii) we again observe the switching of one bit without affecting its direct neighbor.

Finally, although we were unable to resolve individual bits at 3.3 Tbit/in^2 areal density due to the limitations of MFM, we did observe the random distribution of switched bits, which appeared as bright and dark patches when the bits were partially demagnetized (interconnected bits would have had a homogeneous appearance instead). This observation, in addition to the appearance of physical isolation of bits in figure 1(f), suggests that magnetically isolated bits may have been achieved at 3.3 Tbit/in^2 density. Further investigations using higher-resolution MFM tips, techniques, and/or systems are needed to verify the individual switchability of the bits at this density.

In summary, we described a high-resolution fabrication process for patterning magnetic bits without the need for etching or liftoff. By depositing Co/Pd multilayers directly onto resist structures, we demonstrated that magnetic bits could be fabricated up to a density of 3.3 Tbit/in^2. We expect to achieve even higher bit densities by reducing the thickness of the magnetic layer and optimizing the deposition conditions. The concept we describe here is well suited for investigating BPM at the highest possible densities, and could also find use in large-scale manufacturing if the electron-beam lithography step was replaced by (or combined with) scalable self-assembly processes.

Acknowledgments

The authors would like to thank Dr Ramam Akkipeddi for the use of the electron-beam lithography and dual-beam FIB in IMRE through the SERC nano Fabrication Processing and Characterization (SnFPC) facility. This work was supported by the Agency for Science, Technology and Research (A*STAR) in Singapore.

References

[1] White R L 2000 *J. Magn. Magn. Mater.* **209** 1–5
[2] Kryder M H and Gustafson R W 2005 *J. Magn. Magn. Mater.* **287** 449–58
[3] Richter H J 2009 *J. Magn. Magn. Mater.* **321** 467–76
[4] Ross C A 2001 *Annu. Rev. Mater. Res.* **31** 203–35
[5] Ross C A, Smith H I, Savas T, Schattenburg M, Farhoud M, Hwang M, Walsh M, Abraham M C and Ram R J 1999 *J. Vac. Sci. Technol.* B **17** 3168–76
[6] Terris B, Thomson T and Hu G 2007 *Microsyst. Technol.* **13** 189–96
[7] Kikitsu A 2009 *J. Magn. Magn. Mater.* **321** 526–30
[8] Wood R 2009 *J. Magn. Magn. Mater.* **321** 555–61
[9] Stipe B C *et al* 2010 *Nature Photon.* **4** 484–8
[10] Hosaka S, Sano H, Shirai M and Sone H 2006 *Appl. Phys. Lett.* **89** 223131
[11] Choi C, Yoon Y, Hong D, Oh Y, Talke F and Jin S 2011 *Microsyst. Technol.* **17** 395–402
[12] Yang J K W, Cord B, Duan H, Berggren K K, Klingfus J, Nam S-W, Kim K-B and Rooks M J 2009 *J. Vac. Sci. Technol.* B **27** 2622–7
[13] Yang X, Xiao S, Wu W, Xu Y, Mountfield K, Rottmayer R, Lee K, Kuo D and Weller D 2007 *J. Vac. Sci. Technol.* B **25** 2202–9
[14] Park S, Lee D H, Xu J, Kim B, Hong S W, Jeong U, Xu T and Russell T P 2009 *Science* **323** 1030–3
[15] Bigioni T P, Lin X M, Nguyen T T, Corwin E I, Witten T A and Jaeger H M 2006 *Nature Mater.* **5** 265–70
[16] van Dorp W F, van Someren B, Hagen C W and Kruit P 2005 *Nano Lett.* **5** 1303–7
[17] Xiao S, Yang X, Park S, Weller D and Russell T P 2009 *Adv. Mater.* **21** 2516–9
[18] Moneck M T and Zhu J-G 2010 *Proc. SPIE* **7823** 78232U
[19] Morecroft D, Yang J K W, Schuster S, Berggren K K, Xia Q F, Wu W and Williams R S 2009 *J. Vac. Sci. Technol.* B **27** 2837–40
[20] Terris B D 2009 *J. Magn. Magn. Mater.* **321** 512–7
[21] Bita I, Yang J K W, Jung Y S, Ross C A, Thomas E L and Berggren K K 2008 *Science* **321** 939–43
[22] Ruiz R, Kang H M, Detcheverry F A, Dobisz E, Kercher D S, Albrecht T R, de Pablo J J and Nealey P F 2008 *Science* **321** 936–9
[23] Yang X M, Xu Y, Seiler C, Wan L and Xiao S G 2008 *J. Vac. Sci. Technol.* B **26** 2604–10
[24] Austin M D, Ge H X, Wu W, Li M T, Yu Z N, Wasserman D, Lyon S A and Chou S Y 2004 *Appl. Phys. Lett.* **84** 5299–301
[25] Yang J K W and Berggren K K 2007 *J. Vac. Sci. Technol.* B **25** 2025–9
[26] Duan H and Berggren K K 2010 *Nano Lett.* **10** 3710–6
[27] Chen Y J *et al* 2010 *J. Magn. Magn. Mater.* doi:10.1016/j.jmmm.2010.11.094
[28] Chen Y J, Huang T L, Leong S H, Hu S B, Ng K W, Yuan Z M, Zong B Y, Liu B and Ng V 2008 *Appl. Phys. Lett.* **93** 102501
[29] Chen Y *et al* 2010 *IEEE Trans. Magn.* **46** 1990–3
[30] Lu W, Li Z, Hatakeyama K, Egawa G, Yoshimura S and Saito H 2010 *Appl. Phys. Lett.* **96** 143104
[31] Amos N, Ikkawi R, Haddon R, Litvinov D and Khizroev S 2008 *Appl. Phys. Lett.* **93** 203116